

Research Article

Preparation, Characterisation, and Photocatalytic Behaviour of Co-TiO₂ with Visible Light Response

Rossano Amadelli,¹ Luca Samiolo,¹ Andrea Maldotti,² Alessandra Molinari,² Mario Valigi,³ and Delia Gazzoli³

¹ ISOF-CNR, Sezione di Ferrara, Dipartimento di Chimica, Università degli Studi di Ferrara, 44100 Ferrara, Italy

² Dipartimento di Chimica, Università degli Studi di Ferrara, 44100 Ferrara, Italy

³ Dipartimento di Chimica, Università di Roma "La Sapienza", 00185 Rome, Italy

Correspondence should be addressed to Rossano Amadelli, amr@unife.it

Received 1 August 2007; Revised 15 October 2007; Accepted 13 November 2007

Recommended by M. Sabry A. Abdel-Mottaleb

The preparation of cobalt-modified TiO₂ (Co-TiO₂) was carried out by the incipient impregnation method starting from commercial TiO₂ (Degussa, P-25) and cobalt acetate. XPS data show that cobalt is incorporated as divalent ion, and it is likely present within few subsurface layers. No appreciable change in structural-morphologic properties, such as surface area and anatase/rutile phase ratio, was observed. Conversely, Co addition brings about conspicuous changes in the point of zero charge and in surface polarity. Diffuse reflectance spectra feature a red shift in light absorption that is dependent on the amount of cobalt. The influence of cobalt addition on the performance of TiO₂ as a photocatalyst in the degradation of 4-chlorophenol and Bisphenol A is investigated. The results show that the modified oxide presents a higher photoactivity both for illumination with UV-visible ($\lambda > 360$ nm) and visible light ($\lambda > 420$ nm; $\lambda > 450$ nm), and that this enhancement depends on the amount of the added species and on the final thermal treatment in the preparation step. We also show that Co-TiO₂ is a more active catalyst than pure TiO₂ for the reduction of O₂ in the dark, which is an important reaction in the overall photocatalytic processes.

Copyright © 2008 Rossano Amadelli et al. This is an open access article distributed under the Creative Commons Attribution License, which permits unrestricted use, distribution, and reproduction in any medium, provided the original work is properly cited.

1. INTRODUCTION

Recent research in semiconductors photocatalysis is strongly oriented toward the preparation of functional materials that are able to meet specific requirements such as high efficiency and visible light response. These are important issues in the case, for example, of TiO₂ which is an attractive photocatalyst under many aspects but whose use is severely limited by the fact that it absorbs only a relatively small fraction of solar light. On the other hand, from the point of view of photocatalysis for fine chemicals production, illuminated TiO₂ is a too oxidizing system to expect selectivity. In this case, surface tailoring by molecular modification appears to be a viable direction [1].

Different investigations show that doping of TiO₂ by low amounts of foreign elements (both metals and nonmetals) sometimes leads to enhanced photocatalytic activity and to an increase of visible light absorption [2–6].

Metal-doped oxides are also extensively studied for the development of semiconductor nanomaterials with magnetic properties (diluted magnetic semiconductors). This field of research is only broadly related to application of semiconductors in heterogeneous photocatalysis. However, the two disciplines share the necessity of in-depth materials characterisation by a number of physical methods whose results are generally valid independently of the final application.

Among these studies, Co-doped anatase, in particular, is the object of a very large number of publications and review papers [7–14]. Although there seems to be no general consensus on results and interpretation, most authors agree on the fact that (i) Co is present as the divalent form; (ii) Co(II) states are located within the band gap; (iii) cobalt can be located in interstitial positions of the host oxide.

In this paper, we report on the characterisation and photocatalytic behaviour of Co-TiO₂ obtained by the impregnation method, using commercially available TiO₂ and cobalt

acetate as the precursor salt. We discuss, in particular, structural and interfacial properties such as the site occupation and valence state of the metal inside the host oxide, the degree of surface dispersion, changes in the polarity, and acid-basic properties of the surface.

We use the photodegradation of 4-chlorophenol and Bisphenol A to assess the photocatalytic activity of the Co-TiO₂ and TiO₂ and show that the activity of the former is higher, both under UV and visible light irradiation, depending on the degree of doping.

In previous literature work, authors mainly discuss Co-TiO₂ photocatalysts in the context of a more general examination of the effect of different metal dopants [15–20], and the doping degree is generally fixed at one value. Results on the influence of cobalt are contradictory: some authors report an altogether detrimental [15, 16] effect, while, in some cases, cobalt seems to improve photodegradation slightly [17] or selectively for some organic compounds as found by Di Paola et al. [18].

The valence state of Co is also a matter of debate. Thus Wang et al. [19] reach the conclusion that Co³⁺ is more active in bringing about a photoactivity enhancement, in contrast to the works of Choi et al. [15, 16] and of Iwasaki et al. [21]. The paper of the latter authors, on the photodegradation of acetaldehyde, is an interesting work that also examines the effect of the cobalt doping degree. However, neither that paper nor the other cited articles report on the problem of O₂ reduction activation which we deal with in the present publication and to which we attach a considerable importance for an evaluation of the overall activity of photocatalytic processes.

2. EXPERIMENTAL

2.1. Materials

Titanium dioxide P-25 from Degussa was employed in all experiments. The precursor salt used for TiO₂ modification was cobalt acetate obtained from Carlo Erba. The Reichardt reagent (used for measurements of the surface polarity) and all other chemicals were Aldrich pure reagents.

2.2. Apparatus and methods

X-ray diffraction (XRD) patterns in the 2θ angular range from 5° to 60° were obtained by a Philips PW 1729 diffractometer using Cu K α (Ni-filtered) radiation. UV-visible spectra of solutions were recorded on a Kontron spectrophotometer (Uvikon 943), while diffuse reflectance UV-visible spectra (DRS) were recorded in absorbance mode at room temperature in the range 200 nm–2500 nm on a Cary 5E spectrophotometer by Varian Win UV software. Halon was used as reference. The concentration of cobalt in the solution phase was determined by atomic spectroscopy using a Perkin-Elmer, Optica 3100 XL model, instrument.

XPS measurements were carried out with a Leybold-Heraeus LHS10 spectrometer using the Al K α (1486.6 eV) radiation on samples deposited on a gold sheet at a residual pressure in the chamber of 10⁻⁹ Torr. Differential thermal analysis (DTA) data were obtained on a Perkin Elmer

instrument, in the temperature interval from 30° to 800°C at a heating rate of 20°C/min in O₂ flow (50 mL/min), using α -Al₂O₃ as a reference.

Electrochemical experiments were carried out using an EG&G model 273A potentiostat-galvanostat using EG&G software. A conventional three-compartment glass cell was employed where the working electrode compartment had an optical window for illumination. The counter electrode was a Pt gauze and the reference electrode was SCE in all cases.

Photocatalytic experiments have been conducted on suspensions (2 g L⁻¹) or films of the semiconductor whose preparation is described in the following sections. A Helios Italquartz Q400 medium-pressure mercury lamp (15 mW cm⁻²), equipped with suitable cutoff filters, has been employed, and all experiments have been carried out at room temperature (298 ± 1 K) under an atmosphere of 101.3 kPa of O₂.

2.3. Preparation of Co-TiO₂

Cobalt-modified TiO₂ has been prepared by an incipient wetness impregnation method analogous to that described in the literature [22]. In a typical experiment, 0.5 g of TiO₂ (Degussa P-25) was dispersed in 10 mL H₂O that contained the necessary amount of cobalt acetate to obtain the desired percent of doping. The suspension is first sonicated for about 10 minutes to help particles dispersion, then stirred for 2 hours and finally dried in an oven at 100°C for 18 hours. The resulting powder was finely ground in a mortar and calcinated at different temperatures between 100° and 500°C for different times. For comparison, TiO₂ was also treated in the same way but in the absence of added cobalt. The modified oxide is henceforth written as Co-TiO₂ or as Co(*x*%)₂-TiO₂ when the percent (w/w Co/TiO₂) of the added metal needs to be specified. The final powder is greenish while, for comparison, Co-TiO₂ obtained by the hydrolysis of titanium tetraisopropoxide in the presence of cobalt has a yellow/orange colour.

2.4. Preparation of TiO₂ films

Films were prepared from the TiO₂ powders as described in the literature [23]. Pyrex glass was used as the support in photocatalytic experiments. Electrodes were obtained in the same way except that a titanium substrate was used as a support. This was pretreated in hot oxalic acid for 20 minutes before deposition of the TiO₂ films.

3. RESULTS AND DISCUSSION

3.1. Catalyst characterisation

3.1.1. General characterisation

Surface microstructure is highly dependent on the preparation conditions and on posttreatments. Small additions of various metal oxides can also greatly influence (alter) the crystalline morphology as well as the conductivity of the host matrix.

A general investigation of the materials characteristics includes measurements of surface area (BET method), X-ray

diffraction (XRD), and differential thermal analysis (DTA). Surface area measurements were carried out on TiO₂ samples doped with 0.2, 0.5, 1, and 2% w/w and the values obtained ranged from 47 to 49 m²g⁻¹, indicating that the adopted doping procedure does not bring about any surface area change with respect to the pristine oxide (~50 m²g⁻¹). Likewise, XRD spectra of samples with 0.2, 0.5, and 1% Co, collected in the 2θ range 5–60°, showed only peaks due to anatase and rutile, which is expected since the commercial TiO₂ used is well known to be a mixture of the two polymorphs. There is neither an evident change due to Co in the initial anatase/rutile phase distribution nor shift of the diffraction peaks, which can be due to the low resolution in the 5–60 angular range and to the low cobalt content.

DTA experiments gave no indication of phenomena associated with the combustion of organic species (Co acetate has been used as the precursor salt). On the other hand, an exothermic peak, attributable to anatase-rutile phase transformation, was evident in the range from 750° to 800°C.

Invariance of specific surface area facilitates a comparison of the photocatalytic properties of the different materials. More detailed analyses were carried out by XPS and DRS and will be discussed in some detail in the following section.

3.1.2. XPS and DRS measurements

The XPS investigation has provided us with information on both the valence state and the degree of dispersion of cobalt. The Co binding energy (BE) was determined with reference to the Ti2p(3/2) peak at 458.5 eV.

In presence of Co(II), the Co2p region feature two main peaks, Co2p(3/2)-Co2p(1/2), separated by 15.8 eV, and a Co2p(3/2)/Co2p(1/2) intensity ratio of 2. The peaks have shake-up satellites located at ~5.8 eV with higher BE than the main peaks which present a satellite-main peak ratio of about 0.8. Because of covalence and final state effects, the BE of Co(III) is lower than that of Co(II). The magnitude of the chemical shift between the two states is 1.0 eV at most [24]. Owing to the small BE difference and band broadening caused by “multiplet splitting,” the presence of Co(II) or Co(III), or both, cannot be established from the position of the Co2p components alone. A spectral feature that will distinguish between Co(II) and Co(III) is a decrease in the spin-orbit separation and the marked decrease of the satellites, because the main Co(II) peaks present a satellite, whereas the Co(III) peaks do not. As shown in Figure 1(a), in both the Co(1%)-TiO₂ and Co(2%)-TiO₂ samples, the Co2p(3/2) peak is accompanied by the shake-up signal characteristic of Co(II). In addition, for Co(1%)-TiO₂ (curve a), Co2p(3/2) is at 780.8 eV with a shake-up peak separated by 5.7 eV and a satellite-main peak ratio of about 0.8 which indicates the presence of divalent cobalt. For Co(2%)-TiO₂ (curve b) the Co2p(3/2) component is at 780.4 eV with a shake-up separation of 5.2 eV and a satellite-main peak ratio of about 0.45, indicating the presence of Co(II) and Co(III). It can be inferred that in the Co(1%)-TiO₂ sample cobalt is present as Co(II), whereas at increasing cobalt content both Co(II) and Co(III) states are present. The conclusion that Co is present

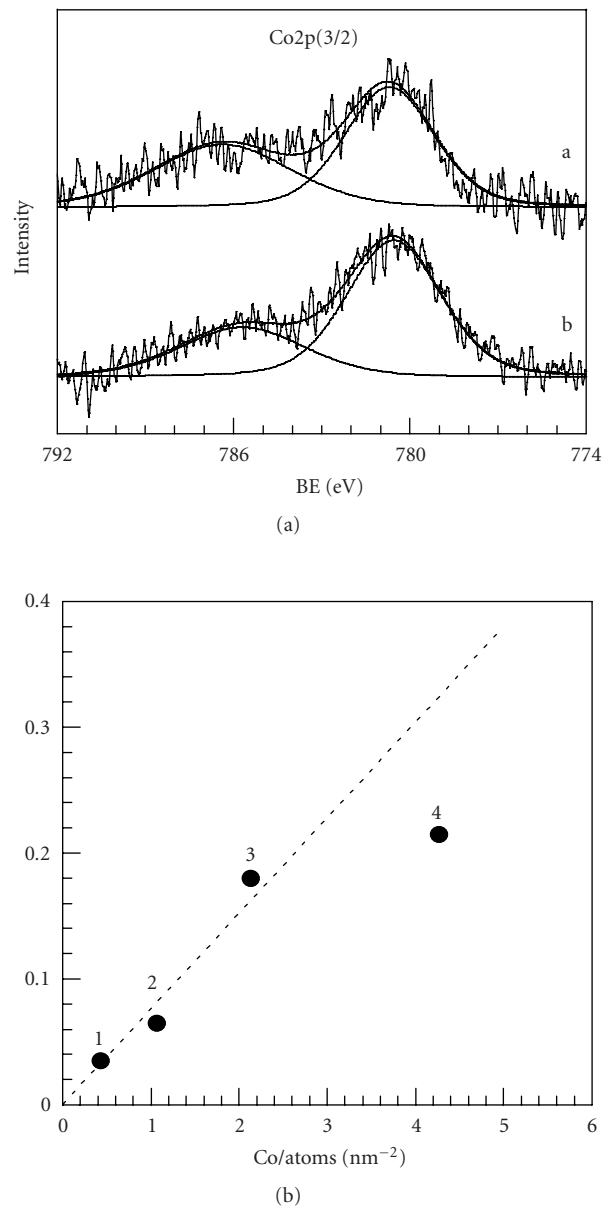


FIGURE 1: (a) XPS spectra in the Co2p(3/2) binding energy region for Co(1%)-TiO₂ (curve a) and Co(2%)-TiO₂ (curve b); (b) ratio of XPS peaks intensity, $I(\text{Co}2p)/I(\text{Ti}2p)$, as a function of the surface concentration of cobalt for Co($x\%$)-TiO₂ with (1) $x = 0.2\%$; (2) $x = 0.5\%$; (3) $x = 1\%$; (4) $x = 2\%$. Full circles are the experimental data and the dashed line refers to calculated values (see text). The final calcination temperature for all samples was 400°C.

in the divalent form is in accord with the above-cited literature [9].

The dispersion degree of cobalt on TiO₂ was determined from the (Co2p/Ti2p) intensity ratios. The plot of the intensity ratio as a function of the surface concentration of cobalt (see Figure 1(b)) shows a deviation from linearity as the content of cobalt increases. For a quantitative evaluation of the surface morphology, the experimental intensity ratios $I(\text{Co}2p)/I(\text{Ti}2p)$ were compared with the values predicted by two

models: the “nonattenuating overlayer over a semi-infinite support” and the “solid solution” models [25]. In the first model, the Co-TiO₂ system was represented as consisting of a nonattenuating dispersed layer of cobalt species on TiO₂ support with semi-infinite thickness:

$$\frac{I_{\text{Co}}}{I_{\text{Ti}}} = \frac{D_{\text{Co}} \sigma_{\text{Co}} s_{\text{Co}}}{D_{\text{Ti}} \sigma_{\text{Ti}} \rho_{\text{Ti}} \lambda_{\text{Ti}}}. \quad (1)$$

In the second model the Co species are considered homogeneously dispersed in the TiO₂ lattice:

$$\frac{I_{\text{Co}}}{I_{\text{Ti}}} = \frac{D_{\text{Co}} n_{\text{Co}} \sigma_{\text{Co}} \lambda_{\text{Co}}}{D_{\text{Ti}} n_{\text{Ti}} \sigma_{\text{Ti}} \lambda_{\text{Ti}}} \quad (2)$$

(ρ_{Ti} indicates the Ti atomic density in the support ($\rho_{\text{Ti}} = 0.29 \cdot 10^{23}$ atoms cm⁻³); D is the instrumental efficiency factor; σ_{Co} , σ_{Ti} are the cross-sections (σ_{Co} , 19.16; σ_{Ti} , 7.91); λ refers to the escape depth of electron (λ_{Ti} , 1.88 nm; λ_{Co} , 1.44 nm); s_{Co} is the Co atomic surface concentration (atoms nm⁻²); and $n_{\text{Co}}/n_{\text{Ti}}$ is the atomic concentration ratio).

The excellent agreement between experimental and calculated values in the Co concentration range 0.2%–1%, as in Figure 1(b), clearly indicates that cobalt is fully dispersed on the surface and within few subsurface layers. Conversely, the intensity ratios calculated by the solid solution model and the experimental ratios disagree (the calculated values are 3–4 times lower than the experimental ones).

The behaviour observed for the Co(2%) sample suggests an aggregation of the cobalt species, likely forming islands or small clusters of Co₃O₄. This is clearly evident in the diffuse reflectance data (see below).

The salient feature of the diffuse reflectance spectra (DRS) displayed in Figure 2 is that Co doping causes a shift of absorption to higher wavelengths (curves a–c). A more in-depth DRS analysis shows interesting details concerning absorption in the visible region (inset in Figure 2) that are useful in establishing the nature of sites occupied by cobalt within the TiO₂ host. For percentages of added Co from 0.2 to 1%, in the wavelength range from 500 to 1000 nm, one can identify three relatively broad peaks close to each other at approximately 530–550 nm, 600–620 nm, and 660–680 nm. For Co(2%)-TiO₂ the spectra (not shown) feature peaks, among others, at 450 nm and 730 nm which are typical of octahedrally coordinated Co(III) [26] indicating a separate phase formation at these degrees of doping, in keeping with the above discussed XPS results.

The pattern, shown in the inset of Figure 2, strongly suggests tetrahedrally coordinated Co and, in fact, the data are comparable with the diffuse reflectance spectra of several Co-modified inorganic materials [27, 28] and of Co-ZnO [29], for which it is well established that the doping metal is divalent and substitutionally occupies Zn tetrahedral sites. However, it is not possible to state that all Co are present in tetrahedral sites since the intensity of transitions attributed to octahedrally coordinated Co is reported to be about two orders of magnitude lower than that for the tetrahedral coordination [29].

The fact that at least a significant amount of Co has a tetrahedral coordination means that the added species which

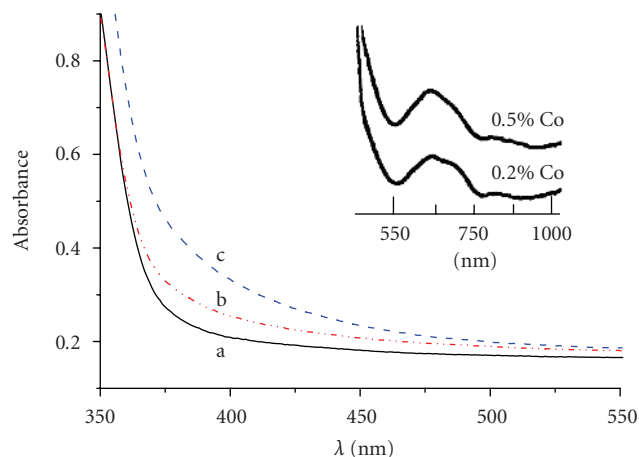


FIGURE 2: Diffuse reflectance spectra of TiO₂ (a); Co(0.2%)-TiO₂ (b); Co(0.5%)-TiO₂ (c). The inset shows measurements on an expanded scale. The final calcination temperature for all samples was 400°C.

entered the lattice, for a few layers, are occupying interstitial positions. This is probably not very surprising considering that our experimental conditions do not involve preparation of Co-TiO₂ by coprecipitation or calcination at high temperatures, which should favour the formation of a homogeneous solid solution with Co in octahedral sites. In this connection, it is interesting to note that among the vast literature on the structure and magnetic properties of Co-TiO₂ prepared by different methods, some studies [10] consider the presence of Co in interstitial tetrahedral sites as well as in octahedral ones plausible; in both cases, the dopant introduces states located about midway within the TiO₂ band gap and causes a raise in the Fermi level [10].

3.1.3. Point of zero charge (PZC) and surface polarity

Oxide surfaces can become charged as a consequence of the ability of coordinated OH groups to undergo hydrolysis. Thus negatively and positively charged surfaces are obtained by the dissociation of acid groups and protonation of basic groups, respectively. The point of zero charge (PZC), corresponding to the condition where no net charge is present on the surface, is an important factor that controls the adsorption of solution species and photocatalytic activity [18].

In the present work, the PZC has been determined by the powder titration method at various values of the solution ionic strength [30]. For undoped TiO₂ (P-25), the value of the PZC is 5.8 as often reported in the literature. In the case of the Co-doped oxide, the PZC is shifted to higher pH values: a value of 7.2 was obtained for TiO₂ doped with 1% Co, as reported earlier [18]. Thus the PZC seems to approach that of bulk Co₃O₄ [30], and one would be led to consider this as a possible cause; it can be ruled out, however, since our DRS and XPS measurements do not indicate the presence of Co³⁺ and of any separate phase formation for Co amounts ≤ 1%.

Quite obviously, the phenomenon we observed originates from changes in the surface properties that can be even

rather subtle, as pointed out in an illuminating work by Contescu et al. on heterogeneity of hydroxyl groups on TiO₂ polymorphs [31]. Among other factors, differences in coordination of –O– and –OH sites to cations, a different proportion of proton binding groups (oxo and hydroxo), variation of the proton-metal distances, and the contribution of different crystal planes (on different planes, terminal oxygen has different acidity) can bring about observable changes in the surface acid/basic behaviour. In contrast to relatively abundant information available for pure TiO₂, investigations on doped TiO₂ appear scanty [18].

From our X-ray data, we have neither evidence of changes in the crystallographic planes intensity upon Co incorporation nor evidence of changes in the TiO₂ unit cell parameters. In this regard, it is worth stressing that Geng and Kim [10] showed that the introduction of interstitial Co into Ti₁₆O₃₂ model clusters leads to volume expansion, and an increased Ti–O bond length can then possibly lead to a more basic behaviour of the surface as discussed by Contescu et al. [31].

In the present work, we also undertook the evaluation of surface polarity, which is an important parameter since changes in polarity (hydrophilicity), along with PZC, can strongly influence the adsorption/desorption equilibria of several compounds and can, consequently, affect the photocatalytic activity.

Experimentally, the quantification of surface polarity is based on suitable indicators which are employed to construct polarity scales. Among these, the $E_T^N(30)$ scale [32], based on the use of Reichardt’s dye, is very well established and can be used to evaluate the polarity of surfaces [33].

Elaboration of our measurements are based on the dimensionless $E_T^N(30)$ scale [34] which ranges from 0 to 1 for nonpolar and very polar surfaces, respectively. The results yielded $E_T^N(30)$ values of 1 for undoped TiO₂ and 0.79 for the Co(0.5%)-doped oxide, clearly indicating a sensible decrease in the surface polarity.

The $E_T(30)$ parameter is correlated to the more accurate Kamlet-Taft scale [35, 36]:

$$E_T(30) = 301.1 + 12.99\pi^* - 2.74\delta + 14.45\alpha + 2.13\beta, \quad (3)$$

where α and β describe the hydrogen-bond acidity and the hydrogen-bond basicity, respectively; δ is a correction factor and π^* is a polarizability/polarity factor. The latter is clearly an important parameter whose evaluation needs separate experiments; however, based on the simple examination of the α parameter, the above-reported decreased acidity of Co-TiO₂ can provide one explanation of the decrease in the $E_T(30)$ or $E_T^N(30)$ compared to undoped TiO₂.

3.1.4. Photoelectrochemical measurements

Oxygen is the common electron acceptor in semiconductor photocatalysis and the study of its reduction bears a high relevance to the optimisation and elucidation of photocatalytic processes [37].

Our electrochemical measurements, in the pH range from 2 to 13, showed that cobalt brings about a shift of the onset of the O₂ reduction process (see Figure 3) toward

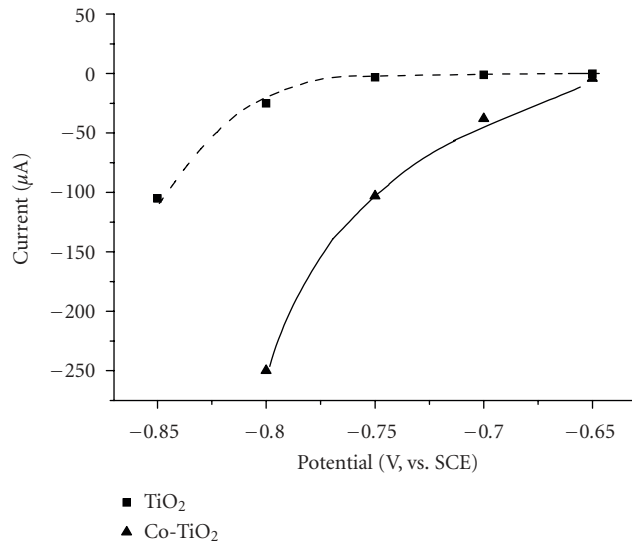


FIGURE 3: Cyclic voltammetry curves for O₂ reduction on TiO₂ and Co(0.5%)-TiO₂ in the dark. Sweep rate: 20 mV s⁻¹. Electrolyte: 0.1 M NaOH. Electrodes geometric area: 2 cm².

more positive potentials, which is ascribed to an electrocatalytic effect. On this basis, one can expect an improvement in the overall photocatalytic processes and, indeed, there is ample literature evidence confirming that coordinated cobalt is an efficient catalyst for oxygen and peroxides activation [38, 39], through pathways involving Co(II) and/or Co(I) species [40].

Our experimental evidence on the effect of added cobalt on peroxide formation during photooxidation processes will be discussed in a separate communication. The results of preliminary investigations show that during photocatalytic experiments, a relatively pronounced accumulation of peroxides in the solution phase is observed with Co-TiO₂ compared to the undoped TiO₂, and this can possibly correlate with the above-reported lower polarity of the former material.

In Figure 4, the photocurrent action spectra plots for TiO₂ and Co-TiO₂, are shown as IPCE (%) [41]:

$$\text{IPCE}(\%) = \frac{1240 \cdot i_{\text{ph}} (\text{mA/cm}^2)}{\lambda (\text{nm}) \cdot I (\text{mW/cm}^2)} * 100, \quad (4)$$

where i_{ph} is the photocurrent and I is the intensity of the light source. The data, obtained from photocurrent-time transients, show a clear response to visible light, in agreement with the DRS data of Figure 2. The lower UV response of Co-TiO₂ compared with TiO₂ (see Figure 4) has been frequently reported in the literature for doped TiO₂ [41, 42] and attributed to the presence of states in the band gap.

The possible charge transfer (CT) processes that occur upon visible light absorption include the dopant centred d-d (MMCT) electronic transitions. In principle, however, metal to ligand (MLCT) and ligand to metal (LMCT) excitation [43, 44] are possible. In our specific case, they would imply electron transfer from the TiO₂ valence band to

Co(II) ($L_{VB}MCT$) and from Co(II) to the conduction band ($ML_{CB}CT$), respectively.

There are investigations on the optical absorption by Co-TiO₂ [11]; however, we want to single out the related, elegant study by Liu et al. [45] because we think it is particularly detailed and informative, considering also that the band gap and band edge positions for ZnO and TiO₂ are similar. Two subbandgap transitions can lead to charge separation: a relatively weak $ML_{CB}CT$ at ~ 715 nm corresponding to Co³⁺ formation and a more intense $L_{VB}MCT$ at higher energy corresponding to Co⁺ formation. According to Schwarz and Gamelin, the Co⁺ state is located in the proximity of the ZnO CB [46].

3.2. Photocatalytic activity

An important goal of the present investigation is the assessment of the effect of cobalt addition on the photocatalytic activity of TiO₂ in the degradation of model organic pollutants. In the previous paragraph, we have drawn attention to the fact that the better catalytic activity of Co-TiO₂ for O₂ reduction, compared with the undoped oxide, offers one good reason to expect improvements in the efficiency of photocatalytic processes. In the following, we examine the photocatalytic activity, for irradiation with both UV and visible light, as a function of additional parameters in the Co-TiO₂ preparation method such as the amount of cobalt and the calcination temperature.

3.2.1. Optimisation of the photocatalytic activity of Co-TiO₂

We have discussed so far the effect of the degree of cobalt doping on the physical characteristics of TiO₂. In this section, we report on the influence of the amount of doping on the photoactivity of Co-TiO₂. Since the final treatment in the preparation of the photocatalysts is calcination, we also carried out a series of experiments aiming to determine the optimal calcination temperature. For this series of correlated experiments, we used 4-chlorophenol as a model substrate because its photodegradation has been extensively investigated and the reaction mechanism is well established [47].

The plots of Figure 5 illustrate the effect of calcination temperature on the time required for mineralization of 4-chlorophenol in suspensions of Co(0.2%)-TiO₂ and of TiO₂ for comparison. Examination of the results reveals that Co-TiO₂ is always more active than the original TiO₂ that was subjected to the same thermal treatment. The best result is obtained for heat treatment at 400 °C for 30 minutes: prolonged heating (>2 hours) at this temperature did not have appreciable effects.

It is important to point out, in this respect, that at this temperature no significant change in the morphology and phase composition is observed for the pure TiO₂ (P-25, Degussa). It is also noteworthy that a low-temperature treatment (100 °C), following TiO₂ impregnation with the cobalt salt, has a negligible influence on the photocatalytic activity (see Figure 5). Moreover, this temperature is not sufficiently high to drive the metal into the lattice, and hence it can be

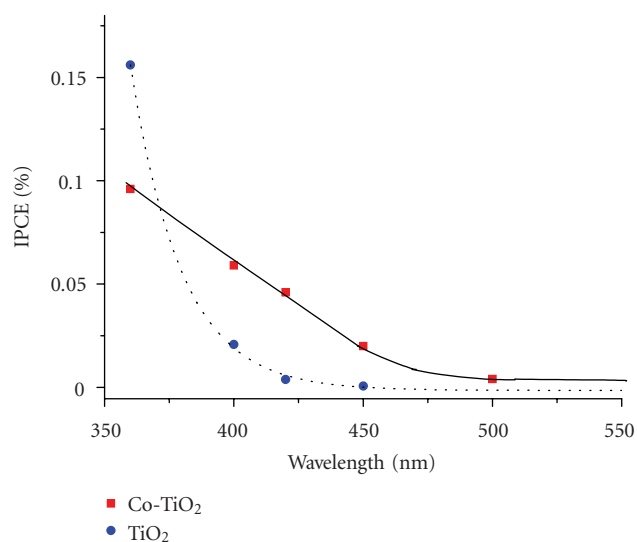


FIGURE 4: Photoaction spectra recorded from photocurrent-time transients using TiO₂ and Co(0.5%)-TiO₂ electrodes in 1M NaClO₄ solutions. Electrodes geometric area: 2 cm².

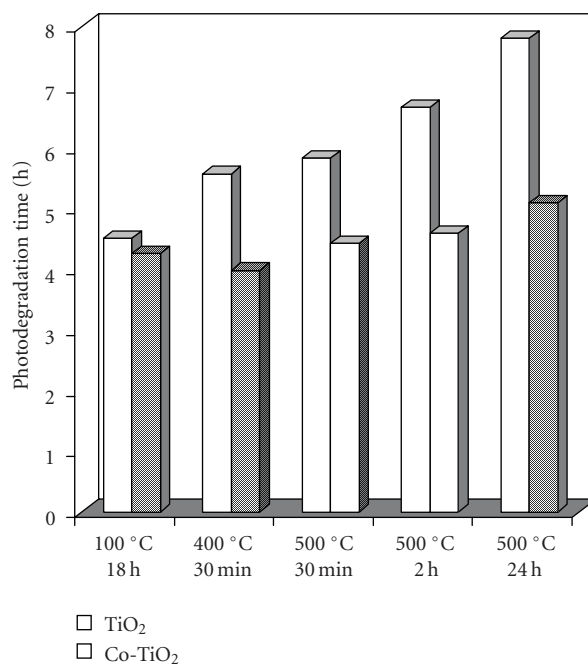


FIGURE 5: Effects of the calcination time and temperature on the time required for the photodegradation of 1 mM 4-chlorophenol in aqueous suspensions of TiO₂ and Co(x%)-TiO₂, where the degree of doping (x%) is 0.2.

concluded that adsorbed Co(II) does not provide active sites for improving the photocatalytic efficiency. This lack of effect is confirmed by photocatalytic experiments carried out in the presence of Co(NO₃)₂ added to the solution.

Experiments for the determination of the photodegradation efficiency of 4-chlorophenol in Co-TiO₂ suspensions were performed as a function of the amount of doping. The

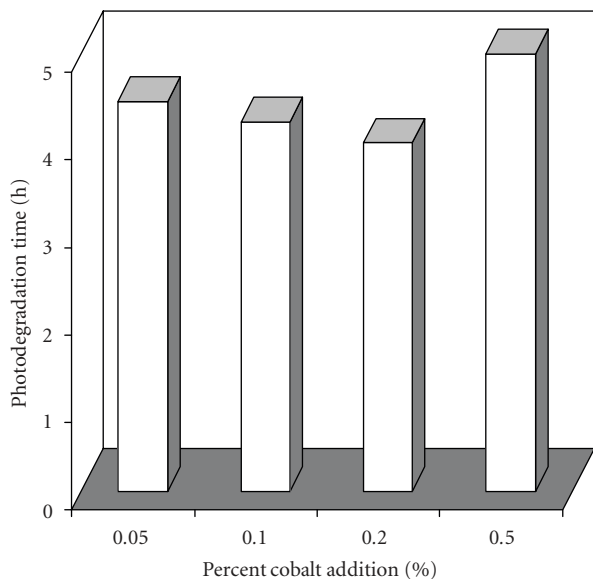


FIGURE 6: Time required for the photodegradation of 1 mM 4-chlorophenol in aqueous suspensions of $\text{Co}(x\%)\text{-TiO}_2$ as a function of the amount of cobalt ($x\%$). The final calcination temperature was 400°C for 30 minutes.

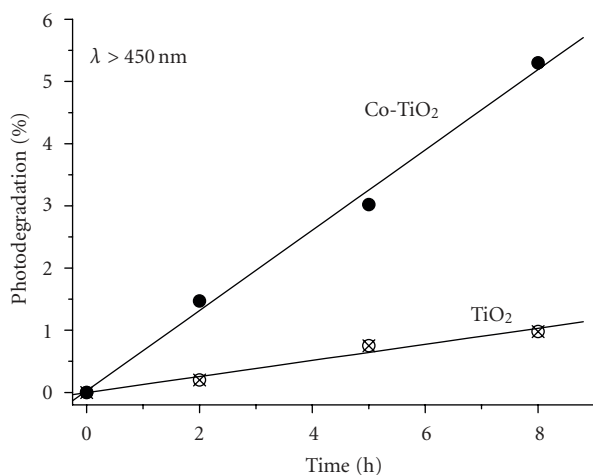


FIGURE 7: Visible light ($\lambda > 450\text{ nm}$) photodegradation of 1 mM 4-chlorophenol as a function of time in aqueous suspensions of TiO_2 and $\text{Co}(x\%)\text{-TiO}_2$, where the degree of doping ($x\%$) is 0.5. The final calcination temperature was 400°C for 30 minutes.

plots in Figure 6 show the effect of a different content in cobalt on the efficiency of 4-chlorophenol photodegradation in Co-TiO_2 suspensions. It is evident that the best results are obtained for a cobalt doping degree of 0.2%.

From the applied point of view, it is often more practical to use photocatalysts in the form of films supported on different substrates such as glass. This is mainly because the use of films avoids the separation of the solid by filtration at the end of experiments, which is a necessary procedure when one uses suspensions. For this reason, we made experiments

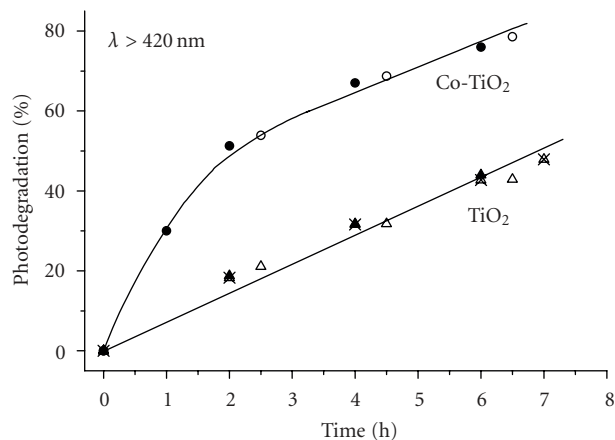


FIGURE 8: Visible light ($\lambda > 420\text{ nm}$) photodegradation of 0.8 mM 2,2'-bis(4'-hydroxyphenyl) propane (Bisphenol A), as a function of time in aqueous suspensions of TiO_2 and $\text{Co}(x\%)\text{-TiO}_2$, where the degree of doping $x\%$ is 0.5. The final calcination temperature was 400°C for 30 minutes.

using glass supported films of TiO_2 and Co-TiO_2 with a different percent of the doping element, again using the photodegradation of 4-chlorophenol as a model reaction. The results showed that in agreement with the reported data for suspensions, Co-TiO_2 is more active than the pristine oxide. Also in accordance with the results of Figure 6, there is an optimum degree of doping for which the photocatalytic activity reaches a maximum that, in this case, turns out to be around 0.5%.

Leaching of cobalt during photocatalytic measurements deserves to be mentioned. For the experimental conditions of Figures 5 and 6, that is, irradiation for ~ 6 hours at a pH close to neutrality, the loss of cobalt as soluble species from $\text{Co}(0.5\%)\text{-TiO}_2$ amounts to 1.44 mg L^{-1} which corresponds to 2.8% of the cobalt concentration that is impregnated into TiO_2 . Measurements at different pH values gave a leaching of 38% and 1.25% at $\text{pH} = 2$ and 10, respectively. It is evident that Co-TiO_2 is not a recommended photocatalyst for applications requiring acidic conditions. For a comparison with literature data, Tayade et al. [17] report a cobalt leaching of 4.6% at $\text{pH} = 5$.

3.2.2. Visible light photoactivity

Both the DRS data of Figure 2 and the photoaction spectra of Figure 4 show that Co-doping causes a red shift in the absorption of light, and in the discussion above we speculated on possible causes (*vide supra*). We thought it was meaningful to carry on experiments in which irradiation is restricted to the visible region ($\lambda > 420$ or 450 nm).

The photodegradation of 4-chlorophenol in Co-TiO_2 suspensions, illuminated with light of wavelength $\lambda > 420\text{ nm}$, confirmed that the doped photocatalyst responds to visible light in a way that depends on the amount of cobalt; the optimal doping degree was found to be 0.5%. The photocatalytic activity of Co-TiO_2 is still good at longer

wavelengths ($\lambda > 450$ nm), but it is interesting to note that undoped TiO₂ still shows residual, albeit low, activity even at these wavelengths (see Figure 7).

We extended our studies on the visible light response of Co-TiO₂ to the photodegradation of 2,2'-bis(4'-hydroxyphenyl) propane (Bisphenol A), a more complex chemical substrate than 4-chlorophenol, that is used for epoxy and polycarbonate resins and is well known to be an endocrine disrupting chemical [48, 49]. Typical results, obtained on irradiation of TiO₂ and Co(0.5%)-TiO₂ suspensions at $\lambda > 420$ nm, are shown in Figure 8. The data confirm the higher photocatalytic efficiency of Co-TiO₂, especially at short irradiation times. As noted for the case of 4-chlorophenol, undoped TiO₂ has an appreciable activity that, in our opinion, is not fully explained. Possible reasons are discussed in a recent paper by Kuznetsov and Serpone [50].

4. CONCLUSIONS

Cobalt-modified TiO₂ (Co-TiO₂) is able to bring about the photocatalytic degradation of pollutants such as 4-chlorophenol and Bisphenol A under both UV and visible light irradiation. The best photoactivity was observed for an amount of cobalt between 0.2% and 0.5% Co/TiO₂ w/w.

Diffuse reflectance measurements indicate that a substantial amount of incorporated Co is present in interstitial positions. XPS measurements show that Co enters the TiO₂ lattice as the divalent species, that it is well dispersed, and that there are no separate cobalt phase formation for percents of added Co < 1%. In this case, the foreign species are likely localized at the surface and within relatively few subsurface layers.

In comparison to pristine TiO₂, Co-TiO₂ features change in the point of zero charge (PZC) toward more basic values and a substantial decrease in the surface polarity. We also show that Co-TiO₂ is a more active catalyst than pure TiO₂ for the reduction of O₂ in the dark.

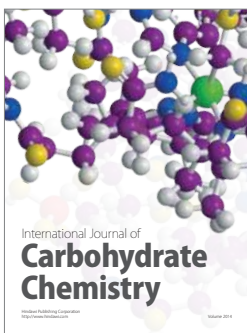
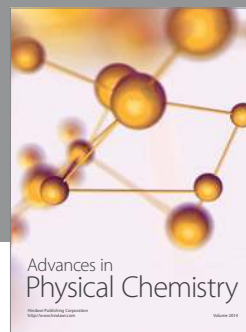
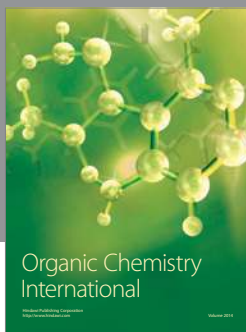
ACKNOWLEDGMENTS

The authors acknowledge the support of CTG-Italcementi, Gambarelli Group, MIUR, and CNR.

REFERENCES

- [1] R. Amadelli, A. Molinari, I. Vitali, L. Samiolo, G. M. Mura, and A. Maldotti, "Photo-electro-chemical properties of TiO₂ mediated by the enzyme glucose oxidase," *Catalysis Today*, vol. 101, no. 3-4, pp. 397-405, 2005.
- [2] K. Mizushima, M. Tanaka, A. Asai, S. Iida, and J. B. Goodenough, "Impurity levels of iron-group ions in TiO₂(II)," *Journal of Physics and Chemistry of Solids*, vol. 40, no. 12, pp. 1129-1140, 1979.
- [3] H. Kato and A. Kudo, "Visible-light-response and photocatalytic activities of TiO₂ and SrTiO₃ photocatalysts co-doped with antimony and chromium," *Journal of Physical Chemistry B*, vol. 106, no. 19, pp. 5029-5034, 2002.
- [4] O. Carp, C. L. Huisman, and A. Reller, "Photoinduced reactivity of titanium dioxide," *Progress in Solid State Chemistry*, vol. 32, no. 1-2, pp. 33-177, 2004.
- [5] M. Anpo, "Preparation, characterization, and reactivities of highly functional titanium oxide-based photocatalysts able to operate under UV-visible light irradiation: approaches in realizing high efficiency in the use of visible light," *Bulletin of the Chemical Society of Japan*, vol. 77, no. 8, pp. 1427-1442, 2004.
- [6] T. L. Thompson and J. T. Yates Jr., "Surface science studies of the photoactivation of TiO₂-new photochemical processes," *Chemical Reviews*, vol. 106, no. 10, pp. 4428-4453, 2006.
- [7] Y. Matsumoto, M. Murakami, T. Shono, et al., "Room-temperature ferromagnetism in transparent transition metal-doped titanium dioxide," *Science*, vol. 291, no. 5505, pp. 854-856, 2001.
- [8] J. M. Sullivan and S. C. Erwin, "Theory of dopants and defects in Co-doped TiO₂ anatase," *Physical Review B*, vol. 67, no. 14, Article ID 144415, 7 pages, 2003.
- [9] W. Prellier, A. Fouchet, and B. Mercey, "Oxide-diluted magnetic semiconductors: a review of the experimental status," *Journal of Physics: Condensed Matter*, vol. 15, no. 37, pp. R1583-R1601, 2003.
- [10] W. T. Geng and K. S. Kim, "Interplay of local structure and magnetism in Co-doped TiO₂ anatase," *Solid State Communications*, vol. 129, no. 11, pp. 741-746, 2004.
- [11] J. D. Bryan, S. M. Heald, S. A. Chambers, and D. R. Gamelin, "Strong room-temperature ferromagnetism in Co²⁺-doped TiO₂ made from colloidal nanocrystals," *Journal of the American Chemical Society*, vol. 126, no. 37, pp. 11640-11647, 2004.
- [12] J. R. Simpson, H. D. Drew, S. R. Shinde, R. J. Choudhary, S. B. Ogale, and T. Venkatesan, "Optical band-edge shift of anatase Ti_{1-x}Co_xO_{2-δ}," *Physical Review B*, vol. 69, no. 19, Article ID 193205, 4 pages, 2004.
- [13] J. M. D. Coey, "Dilute magnetic oxides," *Current Opinion in Solid State and Materials Science*, vol. 10, no. 2, pp. 83-92, 2006.
- [14] R. Janisch and N. A. Spaldin, "Understanding ferromagnetism in Co-doped TiO₂ anatase from first principles," *Physical Review B*, vol. 73, no. 3, Article ID 035201, 7 pages, 2006.
- [15] W. Choi, A. Termin, and M. R. Hoffmann, "Effects of metal-ion dopants on the photocatalytic reactivity of quantum-sized TiO₂ particles," *Angewandte Chemie International Edition*, vol. 33, no. 10, pp. 1091-1092, 1994.
- [16] W. Choi, A. Termin, and M. R. Hoffmann, "The role of metal ion dopants in quantum-sized TiO₂: correlation between photoreactivity and charge carrier recombination dynamics," *Journal of Physical Chemistry*, vol. 98, no. 51, pp. 13669-13679, 1994.
- [17] R. J. Tayade, R. G. Kulkarni, and R. V. Jasra, "Transition metal ion impregnated mesoporous TiO₂ for photocatalytic degradation of organic contaminants in water," *Industrial and Engineering Chemistry Research*, vol. 45, no. 15, pp. 5231-5238, 2006.
- [18] A. Di Paola, E. García-López, S. Ikeda, G. Marci, B. Ohtani, and L. Palmisano, "Photocatalytic degradation of organic compounds in aqueous systems by transition metal doped polycrystalline TiO₂," *Catalysis Today*, vol. 75, no. 1-4, pp. 87-93, 2002.
- [19] J. Wang, S. Uma, and K. J. Klabunde, "Visible light photocatalysis in transition metal incorporated titania-silica aerogels," *Applied Catalysis B: Environmental*, vol. 48, no. 2, pp. 151-154, 2004.
- [20] C. M. Whang, J. G. Kim, E. Y. Kim, Y. H. Kim, and W. I. Lee, "Effect of Co, Ga, and Nd additions on the photocatalytic properties of TiO₂ nanopowders," *Glass Physics and Chemistry*, vol. 31, no. 3, pp. 390-395, 2005.

- [21] M. Iwasaki, M. Hara, H. Kawada, H. Tada, and S. Ito, "Cobalt ion-doped TiO₂ photocatalyst response to visible light," *Journal of Colloid and Interface Science*, vol. 224, no. 1, pp. 202–204, 2000.
- [22] J. Araña, J. M. Doña-Rodríguez, O. González-Díaz, et al., "Gas-phase ethanol photocatalytic degradation study with TiO₂ doped with Fe, Pd and Cu," *Journal of Molecular Catalysis A: Chemical*, vol. 215, no. 1-2, pp. 153–160, 2004.
- [23] C. J. Barbé, F. Arendse, P. Comte, et al., "Nanocrystalline titanium oxide electrodes for photovoltaic applications," *Journal of the American Ceramic Society*, vol. 80, no. 12, pp. 3157–3171, 1997.
- [24] K. Wandelt, "Photoemission studies of adsorbed oxygen and oxide layers," *Surface Science Reports*, vol. 2, no. 1, pp. 1–121, 1982.
- [25] A. Cimino, D. Gazzoli, and M. Valigi, "XPS quantitative analysis and models of supported oxide catalysts," *Journal of Electron Spectroscopy and Related Phenomena*, vol. 104, no. 1, pp. 1–29, 1999.
- [26] Y. Brik, M. Kacimi, M. Ziyad, and F. Bozon-Verduraz, "Titania-supported Cobalt and cobalt-phosphorus catalysts: characterization and performances in ethane oxidative dehydrogenation," *Journal of Catalysis*, vol. 202, no. 1, pp. 118–128, 2001.
- [27] A. A. Verberckmoes, B. M. Weckhuysen, and R. A. Schoonheydt, "Spectroscopy and coordination chemistry of cobalt in molecular sieves," *Microporous and Mesoporous Materials*, vol. 22, no. 1–3, pp. 165–178, 1998.
- [28] H. Hoser, S. Krzyzanowski, and F. Trifiró, "Optical spectra of Co-zeolites," *Journal of the Chemical Society, Faraday Transactions 1*, vol. 71, pp. 665–669, 1975.
- [29] R. Pappalardo, D. L. Wood, and R. C. Linares Jr., "Optical absorption study of Co-doped oxide systems. II," *The Journal of Chemical Physics*, vol. 35, no. 6, pp. 2041–2059, 1961.
- [30] A. Daggetti, G. Lodi, and S. Trasatti, "Interfacial properties of oxides used as anodes in the electrochemical technology," *Materials Chemistry and Physics*, vol. 8, no. 1, pp. 1–90, 1983.
- [31] C. Contescu, V. T. Popa, and J. A. Schwarz, "Heterogeneity of hydroxyl and deuterioxy groups on the surface of TiO₂ polymorphs," *Journal of Colloid and Interface Science*, vol. 180, no. 1, pp. 149–161, 1996.
- [32] C. Reichardt, "Solvatochromic dyes as solvent polarity indicators," *Chemical Reviews*, vol. 94, no. 8, pp. 2319–2358, 1994.
- [33] D. J. Macquarrie, S. J. Tavener, G. W. Gray, et al., "The use of Reichardt's dye as an indicator of surface polarity," *New Journal of Chemistry*, vol. 23, no. 7, pp. 725–731, 1999.
- [34] S. Spange and A. Reuter, "Hydrogen-bond donating and dipolarity/polarizability properties of chemically functionalized silica particles," *Langmuir*, vol. 15, no. 1, pp. 141–150, 1999.
- [35] S. Spange, E. Vilsmeier, and Y. Zimmermann, "Probing the surface polarity of various silicas and other moderately strong solid acids by means of different genuine solvatochromic dyes," *Journal of Physical Chemistry B*, vol. 104, no. 27, pp. 6417–6428, 2000.
- [36] J. L. Jones and S. C. Rutan, "Solvatochromic studies of stationary phases on thin-layer chromatographic plates," *Analytical Chemistry*, vol. 63, no. 13, pp. 1318–1322, 1991.
- [37] A. Maldotti, A. Molinari, and R. Amadelli, "Photocatalysis with organized systems for the oxofunctionalization of hydrocarbons by O₂," *Chemical Reviews*, vol. 102, no. 10, pp. 3811–3836, 2002.
- [38] J. Premkumar and R. Ramaraj, "Photocatalytic reduction of dioxygen by colloidal semiconductors and macrocyclic cobalt(III) complexes in Nafion and cellulose matrices," *Journal of Molecular Catalysis A: Chemical*, vol. 132, no. 1, pp. 21–32, 1998.
- [39] R. S. Drago, "Homogeneous metal-catalyzed oxidations by O₂," *Coordination Chemistry Reviews*, vol. 117, pp. 185–213, 1992.
- [40] S. Leonard, P. M. Gannett, Y. Rojanasakul, et al., "Cobalt-mediated generation of reactive oxygen species and its possible mechanism," *Journal of Inorganic Biochemistry*, vol. 70, no. 3-4, pp. 239–244, 1998.
- [41] J. Y. Shi, W. H. Leng, W. C. Zhu, J. Q. Zhang, and C. N. Cao, "Electrochemically assisted photocatalytic oxidation of nitrite over Cr-Doped TiO₂ under visible light," *Chemical Engineering & Technology*, vol. 29, no. 1, pp. 146–154, 2006.
- [42] T. Lindgren, J. Lu, A. Hoel, C.-G. Granqvist, G. Romualdo Torres, and S.-E. Lindquist, "Photoelectrochemical study of sputtered nitrogen-doped titanium dioxide thin films in aqueous electrolyte," *Solar Energy Materials and Solar Cells*, vol. 84, no. 1–4, pp. 145–157, 2004.
- [43] G. Blaase, "Optical electron transfer between metal ions and its consequences," in *Structure & Bonding*, vol. 76, pp. 153–185, 1991.
- [44] D. A. Schwartz, N. S. Norberg, Q. P. Nguyen, J. M. Parker, and D. R. Gamelin, "Magnetic quantum dots: synthesis, spectroscopy, and magnetism of Co²⁺- and Ni²⁺-doped ZnO nanocrystals," *Journal of the American Chemical Society*, vol. 125, no. 43, pp. 13205–13218, 2003.
- [45] W. K. Liu, G. Mackay Salley, and D. R. Gamelin, "Spectroscopy of photovoltaic and photoconductive nanocrystalline Co²⁺-doped ZnO electrodes," *Journal of Physical Chemistry B*, vol. 109, no. 30, pp. 14486–14495, 2005.
- [46] D. A. Schwartz and D. R. Gamelin, "Reversible 300 K ferromagnetic ordering in a diluted magnetic semiconductor," *Advanced Materials*, vol. 16, no. 23–24, pp. 2115–2119, 2004.
- [47] M. R. Hoffmann, S. T. Martin, W. Choi, and D. W. Bahnemann, "Environmental applications of semiconductor photocatalysis," *Chemical Reviews*, vol. 95, no. 1, pp. 69–96, 1995.
- [48] A. Boscolo Boscoletto, F. Gottardi, L. Milan, et al., "Electrochemical treatment of bisphenol-A containing wastewaters," *Journal of Applied Electrochemistry*, vol. 24, no. 10, pp. 1052–1058, 1994.
- [49] Y. Ohko, I. Ando, C. Niwa, et al., "Degradation of bisphenol A in water by TiO₂ photocatalyst," *Environmental Science and Technology*, vol. 35, no. 11, pp. 2365–2368, 2001.
- [50] V. N. Kuznetsov and N. Serpone, "Visible light absorption by various titanium dioxide specimens," *Journal of Physical Chemistry B*, vol. 110, no. 50, pp. 25203–25209, 2006.



Hindawi

Submit your manuscripts at
<http://www.hindawi.com>

